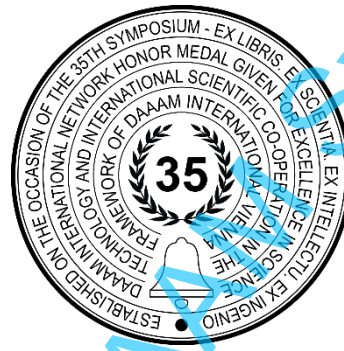


COMPARATIVE ANALYSIS OF ULTRASONIC TESTING SYSTEMS IN FLAW SIZE ESTIMATION

Maria Grozdanic, Morana Mihaljevic & Luka Cvetko



This Publication has to be referred as: Grozdanic, M[aria]; Mihaljevic, M[orana] & Cvetko, L[uka] (2024). Comparative Analysis of Ultrasonic Testing Systems in Flaw Size Estimation, Proceedings of the 35th DAAAM International Symposium, pp.xxxx-xxxx, B. Katalinic (Ed.), Published by DAAAM International, ISBN 978-3-902734-xx-x, ISSN 1726-9679, Vienna, Austria
DOI: 10.2507/35th.daaam.proceedings.xxx

Abstract

One of the primary challenges in ultrasonic testing (UT) is accurately estimating the size of detected flaws, which is essential for evaluating the quality of mechanical parts and their compliance with acceptance criteria. Selecting an appropriate ultrasonic testing system is crucial to enhance measurement reliability and accuracy in flaw sizing, contributing to improved quality assurance. This research aims to evaluate the performance of various UT systems, focusing on different ultrasonic devices and probes, in estimating flaw sizes. The Distance-Gain-Size (DGS) technique with two sizing procedures – DGS mode and DGS diagram (graphically) – was used for flaw size estimation. Measurements were conducted on three calibration blocks with Flat-Bottomed Holes (FBH), representing ideal flaws considering shape and position relative to the sound beam. Based on the measurement results, both DGS procedures provided FBH sizes close to their real sizes when performed with appropriate UT systems. Varying ultrasonic devices in UT systems do not affect the FBH size, while different ultrasonic probes have a significant effect. A lower frequency probe is appropriate for thicker calibration blocks, and both frequency probes are suitable for thinner calibration blocks, with a slight advantage for the higher frequency.

Keywords: flaw sizing; distance-gain-size technique; ultrasonic testing system; ultrasonic device; flat-bottomed hole

1. Introduction

Flaw size estimation is one of the main challenges in ultrasonic testing (UT) [1]. Accurate sizing of detected flaws within a test object is a critical aspect of quality assessment and ensuring structural integrity [2]. When using normal probes, a Distance-Gain-Size (DGS) technique is commonly used for flaw sizing and determining flaw acceptability based on predefined acceptance criteria, which are usually expressed as an Equivalent Reflector Size (ERS). ERS is a clearly defined, repeatable, and reproducible parameter used in standards to establish acceptance criteria [3] against which flaw size is estimated. Therefore, the DGS technique plays a crucial role in adjusting UT systems and improving the accuracy of flaw detection and sizing.

Besides using appropriate sizing technique, reliable characterisation and successful estimation of the detected flaw are affected by several factors, including the UT technique, test part, personnel, and UT system. Therefore, it is important to understand how different factors affect the accuracy of ultrasonic measurements.

Testing techniques can significantly affect the reliability and accuracy of the measurements. Yadav et al. [4] examined the effectiveness and accuracy of pulse-echo and immersion technique on dimensional measurements. They concluded that the immersion technique provides higher precision in thickness measurements than the pulse-echo technique. The immersion technique is less influenced by surface roughness since the transducer is not in direct contact with the test object, while the pulse-echo technique is more practical for field applications. Rungrueng and Prateepasen [5] compared the effectiveness of Phased Array Ultrasonic Testing (PAUT) and Time of Flight Diffraction (TOFD) in detecting and sizing small planar defects in thick wall steel materials. Their study concluded that both techniques have advantages and limitations, and a combined approach utilizing both techniques is recommended for optimal results. The influence of the test part on the accuracy of ultrasonic measurement includes the influence of surface conditions, such as surface roughness [6], and various coatings [7]. Furthermore, the role of the testing personnel is significant as well. Bertovic [8] investigated the impact of human factors on the effectiveness and reliability of various NDT methods, including UT.

Selecting the appropriate UT system is crucial for ensuring the reliability and accuracy of measurements, thereby enhancing the accuracy of ERS estimation. The effectiveness of flaw detection and the accuracy in estimating their sizes are influenced by the components of the selected UT system, which includes the ultrasonic device, ultrasonic probe, couplant, and calibration standard.

Ultrasonic probes vary in frequencies, which is directly related to sensitivity and capability of detecting flaws. Higher frequencies provide better sensitivity, enabling the detection of smaller flaws, but they are more attenuated and less capable of penetrating deeper into the test part. On the contrary, lower frequencies, are less attenuated and capable of deeper penetration but provide lower sensitivity. Thus, selecting a probe requires a compromise between sensitivity and penetration. Yadav [9] investigated how different ultrasonic probe frequencies impact defect detection and characterisation accuracy. Experiments, comparing various probe frequencies, found that higher frequencies (> 10 MHz) are most effective for surface and subsurface defects, while lower frequencies (< 5 MHz) are more reliable for deeper defects. Frequencies between 5 MHz and 10 MHz offer a balance between sensitivity and penetration, making them suitable for general-purpose inspections. In her research, Mihaljević [10] determined that the choice of the ultrasonic probes, considering their parameters (nominal frequency and bandwidth), and the parameters of the selected ultrasonic device (voltage excitation pulse and damping resistance) influences the result of the ultrasonic thickness measurement. Kim and Song [11] studied the effects of couplant in contact ultrasonic testing and compared how different couplant types impact measurement results, noting that high-viscosity couplants generally provide better coupling, resulting in stronger and clearer signals. Using reference standards and calibration procedures helps ensure that ERS measurements are accurate and repeatable. Reference blocks with reflectors like FBHs are commonly used to establish baseline measurements for flaw sizing.

The aforementioned studies underscore the importance of selecting the appropriate UT system to achieve accurate and reliable results. However, while the influences of different UT system components have been investigated, the impact of various ultrasonic devices, and their combination with various probes, on the accuracy of flaw sizing has not yet been investigated.

The main goal of this research is to compare flaw sizing performed with various UT systems, with emphasis on various ultrasonic devices and ultrasonic probes, to determine which UT system provides flaw size estimation closest to the real value. The DGS technique was used for size estimation because DGS provides repeatable and comparable results of flaw sizing, that is ERS. The sizing was performed with the DGS technique using two sizing procedures – DGS mode and DGS diagram. Measurements were performed on three calibration blocks with Flat-Bottomed holes (FBH), which represent flaws of ideal shape and position in relation to the sound beam, to be estimated using the DGS technique.

2. Methods

To evaluate the performance of various UT systems in flaw size estimation, the size of an FBH was estimated. The FBH is a manufacturable version of a theoretical Disc-Shaped Reflector (DSR) used for development of DGS diagrams, making it an ideal flaw for sizing with the DGS technique. A detailed mathematical approach to predict the echo signals from FBH for normal probes is presented in [12]. Estimation of FBH size, expressed as the ERS, is carried out by the HRN EN ISO 16811 standard [13] using the DGS technique. The Pulse-Echo technique was used for calibration and all measurements.

2.1. Ultrasonic testing systems

Eight various UT systems, combining four ultrasonic devices (Figure 1) and two normal ultrasonic probes, were used for estimating FBH sizes.

The UT systems that were used to conduct the measurements consisted of the following components:

- ultrasonic devices: USM 100, USM 36, USM GO and USN 60 (manufacturer: Krautkrämer)
- ultrasonic probes: MB4S and MB5S
- couplant: gel ZGS

- calibration blocks: 5 0088, 5 0100 and 2 0300

To neglect the influence of the ultrasonic device's parameters (energy, voltage, damping and PRF mode) on results, parameters were the same during all measurements. Also, to isolate the influence of probe frequency on FBH size estimation, probes with nominal frequencies of 4 MHz (MB4S) and 5 MHz (MB5S) were selected, having the same probe diameter and frequency bandwidth. Table 1. shows the characteristics of used probes.

Ultrasonic probe	Nominal frequency, MHz	Diameter, mm	Bandwidth, %	Near field, mm
MB4S	4	10	25	15.6
MB5S	5	10	25	20

Table 1. Characteristics of ultrasonic probes MB4S and MB5S



Fig 1. Ultrasonic devices used for sizing FBHs [14]:
a) USM 100; b) USM 36; c) USM GO; d) USN 60

Figure 2 shows various ultrasonic devices used to investigate their accuracy in sizing FBHs in calibration blocks.

2.2. Calibration blocks with Flat-bottomed holes

Flaw size estimation was carried out on three calibration blocks with FBHs. The calibration blocks were made according to the ASTM E428-08 standard, and the data of the characteristic dimensions of the blocks are presented in Table 2.

Calibration block	Thickness, mm	Flat-bottomed hole	
		Diameter, mm	Depth, mm
5 0088	41.15	1.98	22.35
5 0100	44.20	1.98	25.40
2 0300	95.10	0.79	76.20

Table 2. Characteristics of calibration blocks with Flat-bottomed holes

The diameters of FBHs represent their sizes, which will be further used in comparison, as real values. Calibration blocks (Figure 2) were chosen to have FBHs positioned in the far field, that the size estimation using the DGS technique would be reliable.



Fig. 2. Calibration blocks with FBH (from left to right: 5 0088, 5 0100, 2 0300)

Figure 2 shows three calibration blocks with FBHs used in this research. Those blocks are part of a series of blocks containing FBHs of different sizes at different ultrasonic paths, representing reference reflectors, that are usually used to set testing sensitivity.

2.3. Ultrasonic testing systems calibration

For each UT system, a separate calibration was performed using the calibration block 5 0800. Ultrasonic velocities and probe delays, used for further measurements, were determined. The obtained values were also used to carry out measurements on other calibration blocks (5 0100 and 2 0300), considering that all blocks are made of the same material.

Table 3 presents ultrasonic velocities and probe delays determined using block 5 0800 and used for performing measurements with specific UT systems.

Ultrasonic device	USM 100		USM 36		USM 60		USN 60	
Ultrasonic probe	MB4S	MB5S	MB4S	MB5S	MB4S	MB5S	MB4S	MB5S
Ultrasonic velocity, m/s	5882	5879	5833	5879	5837	5879	5880	5876
Probe delay, μ s	0.944	1.707	0.878	1.928	0.793	1.738	0.954	1.759

Table 3. Ultrasonic velocities and probe delays for calibration of different ultrasonic testing systems

After calibrating the UT system, the next step was to estimate the ERSs of FBHs. For this purpose, two measurement procedures of the DGS technique were used.

2.4. Flaw sizing using the Distance-Gain-Size (DGS) technique

The DGS technique can be performed either by using the DGS mode or by graphically reading from the DGS diagram.

Two sizing procedures that use the DGS diagram for flaw sizing are:

- DGS mode which uses DGS diagrams stored in the ultrasonic device and
- Manual use of DGS diagram for graphical estimation of ERS.

Both utilise the same DGS diagrams to estimate the ERS of detected flaws, but they differ in how ERS is determined. When using DGS mode, the ultrasonic device automatically displays flaw size by analysing received signals from flaws, whereas manual use of DGS diagrams involves graphically reading ERS from physical DGS diagrams.

Both sizing procedures are shown in Figure 3.

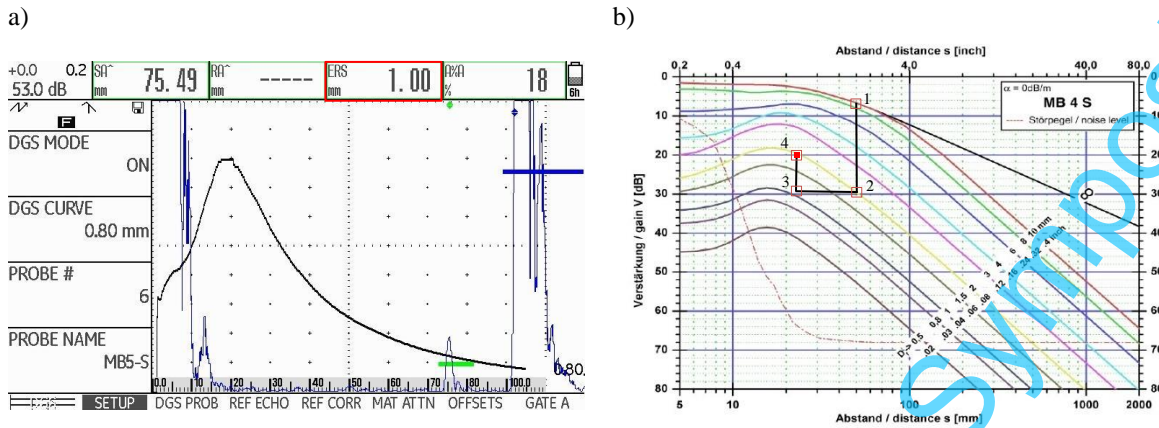


Fig. 3. ERS readings using different DGS technique procedures:
 a) DGS mode; b) DGS diagram - graphically

Figure 3 shows the two sizing procedures that utilise the DGS diagram for flaw sizing. On the left (Figure 3a), an A-scan from the ultrasonic device USM 36 displays the ERS reading. On the right (Figure 3b), a specific DGS diagram for the normal probe MB4S outlines the steps for setting sensitivity (steps 1 and 2) and estimating ERS (steps 3 and 4), where step 4 presents estimated ERS.

DGS mode is a special function integrated into some ultrasonic devices. It utilises DGS diagrams stored in the ultrasonic device for ERS estimation by recording the reference echo (for normal probes is usually the back wall echo from the test object) and recalling the desired curve. Generally, each DGS diagram refers to a specific ultrasonic probe and is unique only to it due to its beam geometry and characteristic values of the ultrasound field. ERS of the detected flaw is read off the screen (Figure 3a). The DGS mode enables a more efficient evaluation of flaw sizes and acceptability. By reducing personnel subjectivity in estimation and improving the reproducibility of results, the process becomes faster and more cost-effective. This integration enhances the accuracy and reliability of flaw sizing and evaluation, providing more accurate measurements and better flaw characterization.

Manual use of DGS diagrams involves graphical estimation of ERS by first recording the reference echo from the back wall of the test object. A gain value (in dB) from the specific DGS diagram is then read and added to the reference gain to achieve the desired sensitivity. Next, the maximum flaw echo signal is identified. If the echo of the flaw is greater or lesser than 80% of the screen height, the gain difference must be added to or subtracted from the point on the diagram. In this diagram, the horizontal axis represents the ultrasound path where the flaw is located in the test object, and the vertical axis shows the working gain. This process identifies a diagram point representing the size of the reference reflector, from which the ERS is read (Point 4 in Figure 3b). If the point lies between two curves, interpolation is required. Manual ERS estimation may introduce errors due to the subjectivity of the testing personnel.

3. Results and Discussion

The sizes of FBHs, expressed as ERSs, were determined using DGS mode and graphically using the physical DGS diagram. Sizing was performed with four UT devices and two normal probes. The estimated ERS values are presented in Table 4 and Table 5. Table 4 displays the results obtained using the MB4S probe, while Table 5 presents the results from the MB5S probe. All values in both tables are expressed in millimetres.

Ultrasonic device	USM 100		USM 36		USM GO		USN 60		Real value
	DGS mode	DGS diagram	DGS mode	DGS diagram	DGS mode	DGS diagram	DGS mode*	DGS diagram	
5 0088	1.95	1.96	1.89	1.95	1.89	1.95	-	1.95	1.98
5 0100	1.90	1.95	1.90	1.94	1.90	1.91	-	1.95	1.98
2 0300	0.79	0.82	0.84	0.84	0.81	0.81	-	0.83	0.79

Table 4. Estimated ERS values in millimetres when testing with normal probe MB4S

Ultrasonic device	USM 100		USM 36		USM GO		USN 60		
Calibration block	DGS mode	DGS diagram	DGS mode	DGS diagram	DGS mode	DGS diagram	DGS mode*	DGS diagram	Real value
5 0088	1.99	2.00	1.98	1.90	1.95	2.00	-	2.00	1.98
5 0100	1.97	2.00	1.97	1.95	1.97	2.05	-	2.00	1.98
2 0300	0.99	0.95	1.00	0.75	0.95	0.95	-	0.85	0.79

Table 5. Estimated ERS values in millimetres when testing with normal probe MB5S

*Ultrasonic device USN 60 has no DGS mode function, therefore only ERS values using the DGS diagram were obtained.

The agreement between the ERS values obtained by the DGS mode and the DGS diagram was analysed. For each calibration block, the deviations between the ERS obtained by the DGS mode and the DGS diagram for each combination of the ultrasonic probe and ultrasonic device are shown graphically in Figure 4.

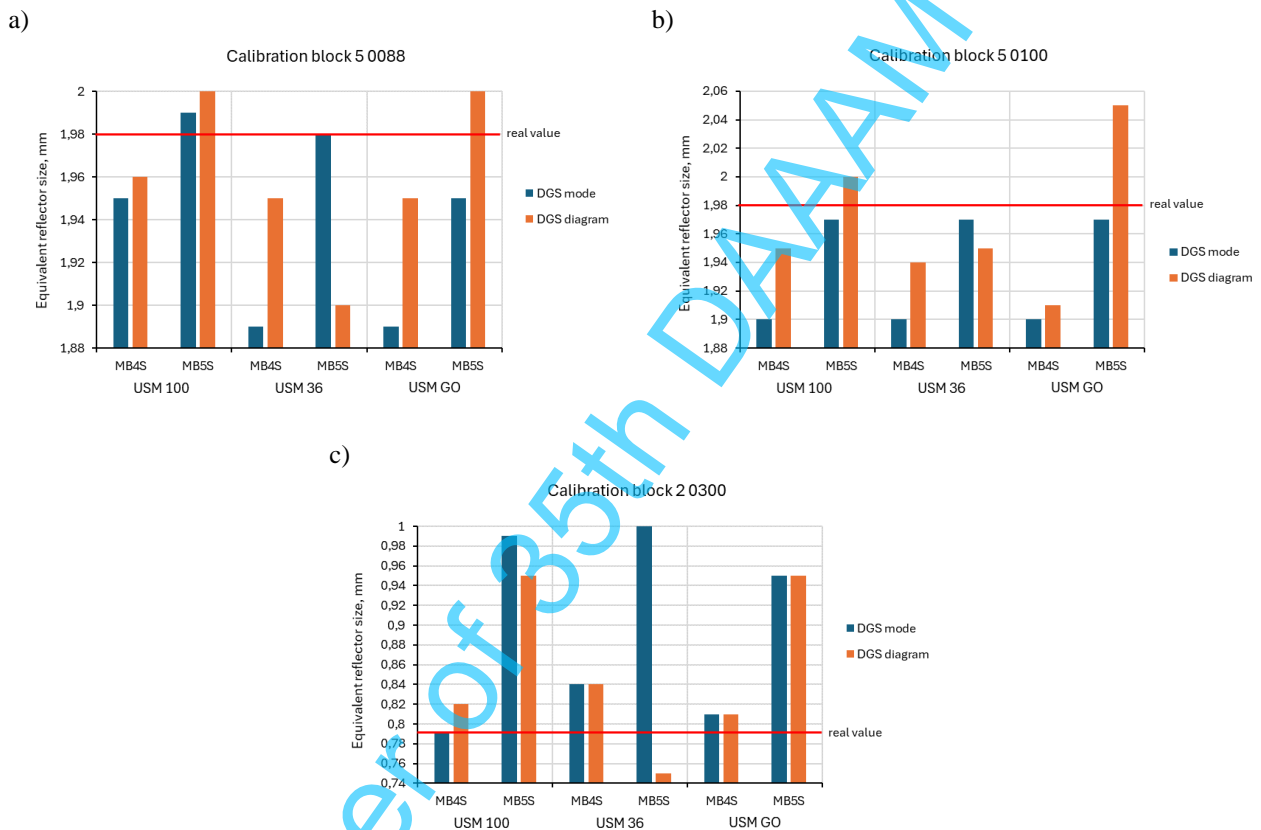


Fig. 4. Differences between ERS values obtained using DGS mode and DGS diagram for various UT systems for calibration blocks: a) 5 0088; b) 5 0100; c) 2 0300

The results in Figure 4 show that different UT systems exhibit varying levels of agreement between the DGS mode and the DGS diagram. Despite the influence of personnel subjectivity in estimating ERS using the DGS diagram, the differences are generally minor, with a maximum deviation of 0.08 mm (4%), excluding the UT system USM 36 – MB5S for calibration block 2 0300. The largest discrepancy between the DGS mode and the DGS diagram is observed when testing calibration block 2 0300 with the UT system USM 36 – MB5S. A deviation of 0.25 mm makes that UT system unreliable for accurate sizing.

For calibration block 5 0088 (Figure 4a) the best assessment between the DGS mode and DGS diagram is achieved with ultrasonic device USM 100 (deviation of 0.01 mm) for both probes. For calibration block 5 0100 (Figure 4b), the difference between results varies depending on the combination of the ultrasonic device and probe. For calibration block 2 0300 (Figure 4c), the differences are smaller compared to the other two blocks, but the results are not always close to the real value.

Figure 4 also provides a visual representation of each measurement deviation from the real value, with more detailed deviation values shown in Figure 5. These deviations will be further discussed.

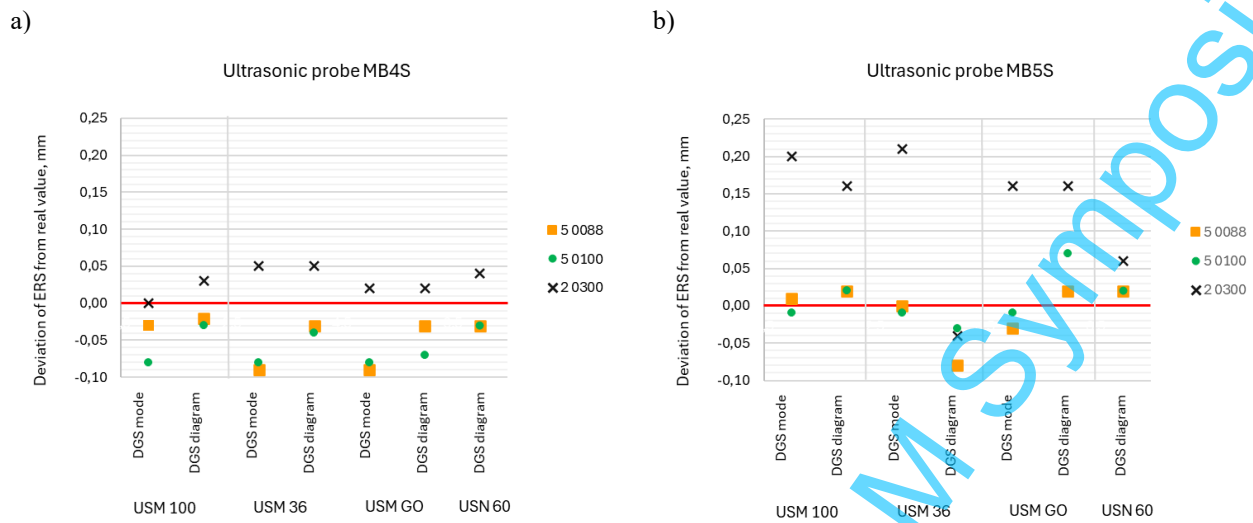


Fig. 5. Deviations of ERS values from real value testing with the ultrasonic probe: a) MB4S; b) MB5S

Figure 5 provides a graphical representation of the deviation of estimated ERS values from real FBH sizes. Figure 5a shows that measurements using the MB4S probe exhibit minimal deviations using all UT systems, with a maximum deviation of 6.3%. Concretely, for calibration blocks 5 0088 and 5 0100, all ERS values are lower than the real values, whereas, for block 2 0300, nearly all results are higher than the real value. Generally, undersizing of flaws, as observed in blocks 5 088 and 5 0100, is more critical to safety than oversizing flaws. Furthermore, in blocks 5 0088 and 5 0100, manual estimation provides more accurate results than devices for all UT systems. Figure 5b indicates that when calibration blocks 5 0088 and 5 0100 are tested with the MB5S ultrasonic probe, estimated values are slightly closer to the real value compared with the values obtained testing with the MB4S ultrasonic probe, and UT system USM 100 – MB5S provides the best results. Significant deviations are visible when testing calibration block 2 0300. Figure 6 provides a more detailed presentation of the deviations from real values. Even though the ultrasonic device USN 60 does not have a DGS mode, it achieves excellent results in estimating ERS using a DGS diagram. For calibration blocks 5 0088 and 5 0100, the deviation from real values is up to 1.5% and for block 2 0300, it is 7.6%, which makes it the most suitable device for evaluating FBH in calibration block 2 0300 when testing with the MB5S ultrasonic probe.

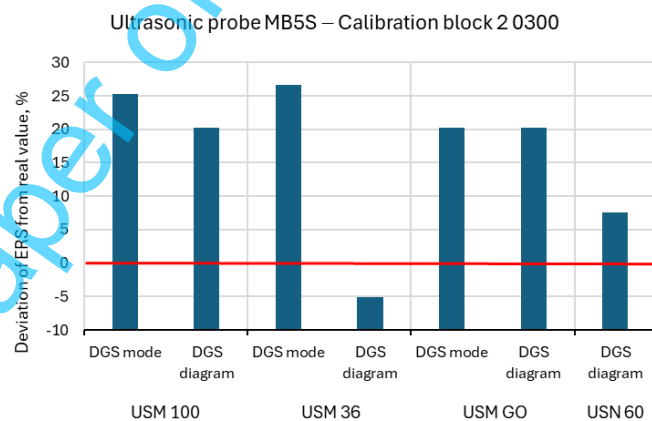


Fig. 6. Deviation of ERS estimated in calibration block 2 0300 testing with ultrasonic probe MB5S

Using the MB5S probe on calibration block 2 0300, regardless of the ultrasonic device and ERS estimation procedures, produces unreliable results with significant deviations. Estimated sizes are significantly larger than the real value. Generally, oversizing flaws may lead to unnecessary repairs or replacements of parts, whose estimated sizes are within the acceptable criteria, which causes unnecessary costs.

4. Conclusion

The influence of various ultrasonic devices (USM 100, USM 36, USM GO and USN 60) and ultrasonic probes (MB4S and MB5S) on the accuracy of flaw sizing using the DGS technique was investigated. Two DGS procedures, DGS mode and DGS diagram, were used for sizing, and the results were compared. Sizing was performed on three calibration blocks, each containing a single FBH. The thinner calibration blocks, respectively 5 0088 and 5 0100, contained FBHs with diameters (sizes) of 1.98 mm at ultrasonic paths of 22.35 mm and 25.40 mm. The thicker calibration block, respectively 2 0300, contained the FBH with a diameter (size) of 0.79 mm at the ultrasonic path of 76.20 mm. The measurement results led to several findings.

For thinner calibration blocks the obtained sizes, expressed as ERS, closely match the real sizes for both sizing procedures and all UT systems. Generally, the maximum deviation was -0.09 mm (4.5%), but most results showed significantly smaller deviations from the real value, with slightly better estimation when using the MB5S probe. For the thicker calibration block, the results obtained when using the MB4S probe were accurate with minor deviations up to 0.05 mm (6.3%). The MB5S probe, however, resulted in significant oversizing with deviations up to 0.21 mm (26.6%).

Finally, it can be concluded that the DGS technique is generally accurate for estimating FBH sizes when used with the appropriate UT system. While the USM 100 device provided insignificant more accurate results, the overall choice of the ultrasonic device did not affect the ERS results. On the other hand, the influence of the probe frequency is significant and greatly affects the measurement results. For measurements on thinner blocks, the MB5S probe gives more accurate results. For measurements on thicker block, the MB4S probe provides results closer to the real value, while the ultrasonic probe MB5S should be avoided due to significant oversizing. Oversizing can be attributed to differences in ultrasonic frequencies; probes with higher frequencies have better sensitivity due to their smaller wavelength but are more attenuated over longer ultrasonic paths. Lower frequencies are more reliable for detecting and estimating sizes over longer ultrasonic paths. Additionally, the human factors in ultrasonic testing should not be overlooked, as the accuracy and interpretation of results highly depend on the skills and experience of the personnel conducting the measurements.

Further research will test additional calibration blocks with varying FBH sizes and ultrasonic paths to perform a more detailed analysis of the influence of UT systems on size estimation. That will help to refine the understanding of the impact of different ultrasonic devices and probe frequencies on flaw sizing accuracy using the DGS technique.

5. References

- [1] Dwivedi, A.; Gupta, R. K.; Varma, R. K. & Narayanan, K. S. (2016). Effect of Processing and Microstructure on Ultrasonic Response of Aerospace Alloys: An Overview. *Russian Journal of Nondestructive Testing*, Vol. 52, No. 12, 703-709, ISSN 1061-8309
- [2] Kim, H. J.; Song, S. J. & Kim, Y. H. (2003). Quantitative Approaches to Flaw Sizing Based-On Ultrasonic Testing Models, *Proceedings of Review of Progress in Quantitative Nondestructive Evaluation*, Thompson, D. O. and Chimenti, D. E. (Ed.), pp. 703-710, AIP Conference Proceedings, Bellingham, DOI: 10.1063/1.1570205
- [3] Krautkramer, J: *Ultrasonic Testing Level 2*
- [4] Yadav, K.; Yadav, S. & Dubey, P.K. (2021). A Comparative Study of Ultrasonic Contact and Immersion Method for Dimensional Measurements. *MAPAN-Journal of Metrology Society of India*, Vol. 36, No. 2, 319-324
- [5] Rungrueng, C. & Prateepasen, A. (2019). Comparison of Detection and Height Sizing Ability of Planar Defect in Thick Wall Weld Steel Between PAUT and TOFD Techniques. *International Journal of Recent Engineering Research and Development*, Vol. 4, Issue 4, 21-38, ISSN 2455-8761
- [6] Rodriguez, E. (2003). Effect of Surface Roughness in Ultrasonic Testing (Pulse-Echo by Direct Contact) in AISI/SAE 4340 Steel Samples. Available from: <https://www.ndt.net/article/ecndt02/254/254.htm>, Accessed: 2024-07-01
- [7] Mihaljevic, M[orana]; Cajner, H[rvoje]; Markucic, D[amir] & Kozic, K[arlo] (2018). Coating Influence on Ultrasonic Thickness Measurement Result, *Proceedings of the 29th DAAAM International Symposium*, pp.0341-0346, B. Katalinic (Ed.), Published by DAAAM International, ISBN 978-3-902734-20-4, ISSN 1726-9679, Vienna, Austria DOI: 10.2507/29th.daaam.proceedings.049
- [8] Bertovic, M. (2015). *Human Factors in Non-Destructive Testing (NDT): Risks and Challenges of Mechanised NDT*, Ph.D. Dissertation, Technical University Berlin, Berlin, Germany
- [9] Yadav, K.; Dhiman, N.; Yadav, S. & Dubey, P. K. (2022). Effect of Probe Frequency on Defect Evaluation in Ultrasonic Non-Destructive Testing, New Delhi, Yadav. S. et al. (Ed.), pp. 14-17, New Delhi
- [10] Mihaljevic, M. (2015). Measurement uncertainty estimation of the ultrasonic thickness measurement, Ph.D. Dissertation, Department of Quality, Doctoral thesis, University of Zagreb, Faculty of Mechanical Engineering and Naval Architecture, Zagreb, Croatia
- [11] Kim, Y.; Song, S. J.; Lee, S. S.; Lee, J. K.; Hong, S. S. & Eom, H. S. (2002). A Study of the Couplant Effects on Contact Ultrasonic Testing. *Journal of the Korean Society for Nondestructive Testing*, Vol. 22, No. 6, 621-626
- [12] Danilov, V.N. (2007). Calculation of Echo Signals from a Flat-Bottom Hole for Normal Probes. *Russian Journal of Nondestructive Testing*, Vol. 43, No. 11, 724-732, ISSN 1061-8309
- [13] *Non-destructive testing – Ultrasonic testing – Sensitivity and range setting (ISO 16811:2012)*, International Organization for Standardization, 2012
- [14] <https://www.bakerhughes.com/waygate-technologies>, Accessed: 2024-07-04